sciendo

POLISH MARITIME RESEARCH 4 (112) 2021 Vol. 28; pp. 107-121
10.2478/pomr-2021-0053

RESEARCH ON THE APPLICATION OF COLD ENERGY OF LARGE-SCALE LNG-POWERED CONTAINER SHIPS TO REFRIGERATED CONTAINERS

Yajing Li[1]
Boyang Li[1]
Fang Deng[1]
Qianqian Yang[1]
Baoshou Zhang[2]
[1] College of Electromechanical Engineering, Qingdao University of Science and Technology, China
[2] School of Aerospace Engineering, Tsinghua University, China
* Corresponding author: *qdlby@126.com (B. Li)*

ABSTRACT

With the aim of considering the problem of excess fuel cold energy and excessive power consumption of refrigerated containers on large LNG-powered container ships, a new utilisation method using LNG-fuelled cold energy to cool refrigerated containers in cargo holds is proposed in this study, and the main structure of the cold storage in the method is modelled in three dimensions. Then, combined with the different conditions, 15 different combination schemes of high temperature cold storage and low temperature cold storage are designed to utilise the cold energy of LNG fuel, the exergy efficiency and cold energy utilisation rate calculation model of the system is established. The simulation tool 'Aspen HYSYS' is used to simulate and calculate the exergy efficiency and cold energy utilisation rate of the system under 15 combinations, verifying the feasibility of the scheme. According to the characteristics of such a ship's cross-seasonal navigation routes and the number of refrigerated containers loaded in different ports, the combination schemes of the number of low-temperature cold storage and high-temperature cold storage are selected. Thus, the average exergy efficiency and cold energy utilisation rate of the whole line is obtained, which proves that LNG-powered container ships could effectively utilise the cold energy of LNG. By calculating the total electric energy consumed by refrigerated containers on the whole sailing route, before and after the adoption of the LNG cold energy method, it is found that the adoption of this new method can promote the realisation of energy saving and emission reduction of ships.

Keywords: LNG-powered container ship,LNG cold energy utilization,Refrigerated container,Cold storage

INTRODUCTION

At present, many large ships mainly use reliable fuel oil as fuel and combustion produces a large amount of harmful gases, such as nitrogen oxides and sulphur oxides, causing serious atmospheric pollution [1-2]. In response to increasingly severe environmental problems [3], the IMO (International Maritime Organization) has put forward more and more stringent requirements on ship exhaust emissions [4-7]; this has prompted ship owners to urgently find cleaner, more environmentally friendly, alternative fuels [8-9].

In recent years, LNG (liquefied natural gas) has been used as a ship fuel because of its clean, efficient, and pollution-free advantages [10, 11]. Rui Zhao et al. [12] proposed the use of hydrogen natural gas and diesel fuel engines on ships. Experiments and numerical simulations have verified that this type of engine has good combustion performance and can also reduce environmental pollution but, currently, dual-fuel diesel engines are mainly used, with LNG as the main fuel, which can also greatly reduce pollutant emissions. Such ships are called 'LNG powered ships'. With the increase in people's awareness of environmental protection, the number of LNG powered ships has gradually increased, especially in large container ships. Before the LNG fuel is sent to the main engine for combustion, it needs to be vapourised to the supply temperature and then used in the main engine of the ship.

During the process of vapourising the LNG fuel from -162°C to normal temperature (20°C~40°C), each kilogram of LNG fuel can release 830kJ ~ 860kJ of cold energy [13, 14]. At present, when LNG is heated and vapourised, most of the cold energy is discarded with seawater and air and a large amount of cold energy cannot be used, resulting in a lot of wasted energy [15, 16]. It will also cause indirect pollution and harm to the surrounding seas due to the cold energy, therefore, industry needs to focus research on how to make full use of this part of the cold energy.

Currently, LNG cold energy can be used in seawater desalination, air separation, and Rankine cycle power generation, etc. [17-19].

Sang Hyun Lee et al. [20] proposed a new type of process that uses LNG cold energy for seawater desalination and can generate electricity, which can solve the energy-intensive problem of traditional seawater desalination, and optimise the economic analysis of this new process. Compared with traditional seawater desalination methods, this method has higher energy efficiency. Babu et al. [21] designed a hydrate desalination process that can use the cold energy produced by LNG vapourisation to improve the recovery rate of fresh water through an innovative hydrogenation process. Experiments show that the water recovery rate can reach 34.85%. Jing Sun et al. [22] proposed a method for seawater freezing and desalination using LNG cold energy for LNG receiving stations. It has been verified that this method has high heat transfer efficiency, but the ice production efficiency of the fluidised bed ice-maker is affected by the ability of particles to remove ice crystals. Therefore, the technology needs to continue to be optimised. Cao et al. designed and simulated the process of freezing desalination using LNG cold energy on a flake ice maker, established a kinetic model of the freezing section and performed numerical simulations. The results showed that a 1 kg equivalent of LNG cold energy can obtain approximately 2 kg ice melt water [23]. In the 1970s, Cravalho et al. proposed a zero-energy, theoretical system for recovering LNG cold energy to produce fresh water. The system included a heat engine, heat pump, LNG heat exchanger and two seawater heat exchangers. The maximum theoretical fresh water output of the system was about 6.7 kg (water) kg $(LNG)^{-1}$ [24].

Using LNG cold energy in the air separation process can realise part of the cold energy recovery [25]. Yamanouchi, Nagasawa, and Wu all [26-28] proposed a process for cryogenic air separation using the cold energy released during the LNG vapourisation stage and verified the feasibility and rationality of the process, saving energy. LNG cold energy can also be used for the recovery of light hydrocarbons. Zhang used the cold energy in the LNG regasification process to recover light hydrocarbons and optimised the cold energy utilisation rate (CUR) and ethane recovery rate (ERR). Gu designed an LNG light hydrocarbon recovery process by adopting the method of partial condensation of natural gas and recycling the feed to improve the purity of light hydrocarbon products, such as ethane. Gao et al. used cold energy to improve the LNG light hydrocarbon recovery process. They made the demethanizer work under high pressure (about 4.5 MPa), which can compress the thin natural gas product to pipeline pressure and reduce power consumption.

There have also been many studies on using LNG cold energy for Rankine cycle power generation. Koo studied a new solution for recovering LNG cold energy from LNG-powered ships, replacing the typical LNG fuel supply system with an organic Rankine cycle (ORC) system to recover the cold energy of LNG, which has more advantages than the traditional Rankine cycle. Big advantage. Six different ORC systems were proposed and optimised to verify the economic feasibility of the system [32-34]. Zhen Tian et al. proposed a parallel two-stage organic Rankine cycle (PTORC) system driven by an LNG fuel ship's waste heat. Through simulation and analysis, it is concluded that the PTORC system can effectively utilise the LNG cold energy and waste heat of dual-fuel ship engines [35]. Sun proposed a power generation system that uses the combination of waste heat from the main ship engine's flue gas and LNG low-temperature cold energy, and then analysed and simulated the system, using genetic algorithms to optimise the relevant parameters that affect the efficiency of the system. The exergy efficiency of the low-temperature Rankine cycle power generation system has been significantly improved [36]. Xu proposed a new type of power generation system that uses LNG cold energy for Rankine cycles, to reduce heat exchanger exergy loss, optimise the system, and improve the exergy efficiency of the system [37]. Liang et al. proposed a new LNG cold energy utilisation system that combines cold, heat and electricity. The system consists of a gas turbine, 4 Rankine cycles and a natural gas direct expander. The recovery and utilisation of the cold energy of LNG can improve the thermal efficiency and exergy efficiency of the system [38]. Fernández et al. proposed to capture BOG energy in LNG ships and produce high-energy and zero-emission hydrogen as a fuel for ships, using the cold energy of LNG fuel during the storage of hydrogen, thereby reducing the space occupied by hydrogen storage on the ship; the power consumed by the compressor when compressing hydrogen is calculated [39].

At present, the load of seawater desalination, air separation, air conditioning, etc. is relatively small, and only a small part of the cold energy is used, most of them being applied on land. Even if it is applied to ships, most of the cold energy released by LNG is still not used. In addition, the Rankine cycle power generation system is only widely used to drive steam turbines on LNG carriers. Because of its complex system structure, management requirements on ships are relatively high, and it is not widely used on other types of ships. Therefore, it is particularly important to find an efficient utilisation scheme of LNG cold energy that can be applied on ships.

With the widespread application of LNG fuel, large container ships took the lead in opening the prelude to LNG-powered ocean-going ships. This is not only because container ships have a high speed and consume a lot of fuel, but also because large container ships usually have a large number of refrigerated containers, which can reach more than 2,000, resulting in a large electrical load for refrigerated containers.

More importantly, LNG-powered container ships consume a lot of LNG fuel and release a lot of cold energy. Because the above-mentioned LNG cold energy utilisation has some shortcomings, there is a problem of excess LNG cold energy on such ships, and it happens that the refrigerated containers carried by the ships urgently need a large amount of cold energy. Therefore, it is proposed to use LNG cold energy for ship refrigerated containers. The specific method is to install an insulation layer in the cargo hold near the midship (a new type of cold storage). The goods that need to be refrigerated should be put into containers, which are placed in the new type of cold storage, using the refrigerant to transfer the LNG cold energy to the cold storage, and then the containers are cooled, to achieve the effect of refrigerated containers. Aspen HYSYS software was used to simulate the process, which proved the feasibility of the above plan.

STRUCTURAL MODEL OF THE COLD STORAGE

SELECTION OF THE PARENT SHIP

In order to realise the full and effective use of LNG cold energy on large container ships, this study is based on the world's largest container ship 'CMA CGM JACQUES SAADE' which is to be launched in 2020, as the parent ship. The ship can carry 23,000 standard containers (TEU), as shown in Fig. 1.

Fig. 1. 'CMA CGM JACQUES SAADE' LNG-powered container ship

The parent ship uses a CMD-WinGD 12*92DF dual-fuel low-speed diesel engine as the main engine of the ship. The main engine has a large power of 63,840 kW. Therefore, the LNG fuel consumption is high and releases more cold energy. In addition, the ship uses more electrical equipment and power consumption is large, with 6 generator sets; the specific parameters are shown in Table 1. The power of the refrigerated container is the average power of the refrigerated container obtained through experimental measurement during continuous operation.

Tab. 1. Related parameters of 'CMA CGM JACQUES SAADE'

Parameters	Value	Parameters	Value
Length overall (m)	399.9	Deadweight (ton)	216900
Breadth moulded (m)	61.3	Main engine power (kW)	63840
Depth (m)	33.5	Number of refrigerated containers (40 feet)	2200
Draft (m)	14.5	LNG fuel tank volume (m3)	18600
Generator power (kW)	38404×4	Average power of refrigerator (40 feet) (kW)	4.8-5.8
	43202×2	Average speed (knot)	21.55

The parent ship selected in this study uses LNG as fuel and the specific composition of the LNG is shown in Table 2. When the container ship sails at 70% of the rated power of the main engine, through calculation, it can be concluded that the container ship can consume 6497 kg of LNG fuel per hour. The cold energy released per hour, during the LNG vapourisation process, can be calculated as $5.52*10^6$ kJ, it can be seen that the container ship will release a large amount of cold energy during normal navigation.

Tab. 2. LNG composition

Component	Methane	Ethane	Propane	Iso-butane	N-butane	Nitrogen	Iso-pentane
Percentage	0.9390	0.0326	0.0069	0.0012	0.0015	0.0179	0.0009

OVERALL DESIGN SCHEME OF THE COLD ENERGY UTILISATION SYSTEM

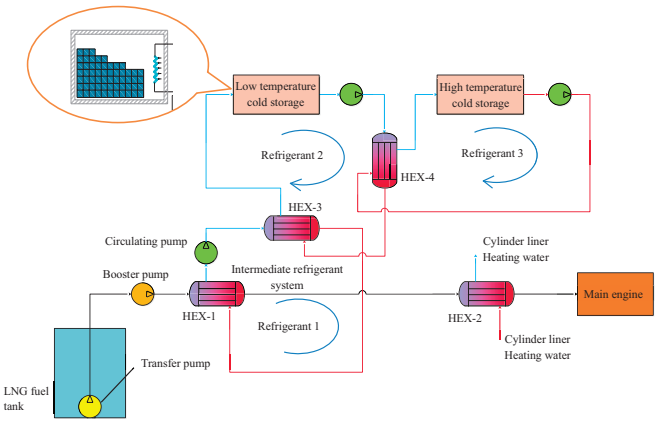

Fig. 2. LNG cold energy utilisation system

Because the temperature of LNG fuel is low, reaching -162°C, and the minimum design temperature of the cold storage is only -20°C, the heat exchange temperature difference is large and the selection of refrigerant is difficult. Excessive heat exchange temperature difference will cause a lot of waste of LNG cooling exergy. Therefore, when designing the system, an intermediate refrigerant system was added, as shown in Fig. 2, where the circulating refrigerant is refrigerant 1. The system is divided into an intermediate refrigerant system, a low temperature cold storage system, a high temperature cold

storage system, and the water heating system of the cylinder liner. The intermediate refrigerant system, low temperature cold storage system, and high temperature cold storage system adopt the cold energy cascade utilisation method. LNG first passes through the LNG heat exchanger HEX-1, transfers the cold energy to refrigerant 1 in the intermediate refrigerant system, and then uses the jacket water to heat and vapourise it through the LNG heat exchanger, HEX-2, and send it to the ship's main engine for combustion. Refrigerant 2 (in the low-temperature cold storage system) and refrigerant 1 (in the intermediate refrigerant system) exchange cold energy through HEX-3 and the high-temperature cold storage system exchanges cold energy through refrigerant 3 and refrigerant 2 in the low-temperature cold storage through HEX-4. Finally, by using the heat of the cylinder liner to heat the water, the remaining cold energy is consumed so that the LNG is completely vapourised to the intake temperature of the main engine of the ship.

DESIGN OF THE NEW COLD STORAGE MODEL

Refrigerated containers usually include low-temperature refrigerated containers and high-temperature refrigerated containers. Low-temperature refrigerated containers usually transport some low-temperature cargo, such as meat, fish and other foods. The temperature is usually -18°C to -20°C. High-temperature refrigerated containers usually transport fruit, vegetables and other cargo; the temperature is usually between 0°C and 5°C. Most of the refrigerated containers are equipped with refrigeration equipment and insulation layers, which not only increases the investment and construction cost of the ship, but also increases the power consumption caused by refrigeration of the refrigerated containers.

In order to meet the temperature requirements of low-temperature refrigerated containers and high-temperature refrigerated containers, low-temperature cold storage and high-temperature cold storage are divided. The cold storage is set in the cargo hold in the middle of the ship and the cargo hold is provided with an insulation layer. The reason for placing the cold storage in the middle of the hull is that the cargo hold has a more regular shape than the cargo hold on the bow and stern and can accommodate more containers. This method can not only put refrigerated containers in the cargo hold, it can also be put into ordinary containers but, more importantly, it allows an ordinary container store refrigerated or frozen goods like a refrigerated container. This not only improves the energy utilisation rate of the ship, but also reduces the increase in refrigeration caused by the refrigerated container during maritime transportation. The load on the ship's power grid can save ship operating costs. After calculation, each cold storage can accommodate 528 TEUs. The dimensions of the cold storage are shown in Table 3. Fig. 3 is a three-dimensional model of one of the cold storages.

Tab. 3. Relevant parameters of cold storage

Parameters	Length (m)	Width (m)	Height (m)
Value	12.60	54.67	31.69

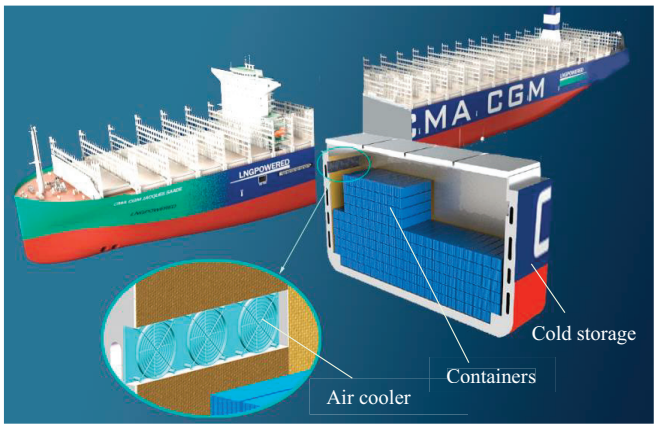

Fig. 3. Model diagram of the new cold storage

SCHEME DESIGN

CALCULATION OF COOLING CAPACITY REQUIRED BY COLD STORAGE

In order to realise the utilisation rate of LNG cold energy on LNG-powered container ships, it is necessary to calculate the cooling load of the cold storage in the design scheme.

The specific calculation method for each cold storage is as follows. The total cold consumption is:

$$\dot{Q} = \dot{Q}_1 + \dot{Q}_2 + \dot{Q}_3 + Q_4 \quad (1)$$

where $\dot{Q}_1$ is the heat flow rate between the cold storage and its surrounding environment (W); $\dot{Q}_2$ is the heat flow rate of the goods in the cold storage (W); $\dot{Q}_3$ is the heat flow rate generated when the cold storage is opened for ventilation (W); and $\dot{Q}_4$ is the equipment or operator heat flow rate (W).

Heat flow rate between cold storage and external environment $\dot{Q}_1$

The heat flow rate between the cold storage and external environment is calculated according to the following formula:

$$\dot{Q}_1 = KF\Delta T \quad (2)$$

where K is the heat transfer coefficient of the cold storage wall, W/m²·K; F is the heat transfer area of the cold storage, m²; and ΔT is the temperature difference between the ambient temperature and the storage temperature, K. The temperature of the outer wall of the cold storage is 30°C in summer, 5°C in the winter, and 15°C in the spring and autumn.

Cargo heat flow rate of cold storage $\dot{Q}_{2L}$, $\dot{Q}_{2H}$,
Low-temperature cold storage usually stores some low-temperature cargo, such as meat, fish and other foods. For the heat flow rate of low-temperature cold storage goods:

$$\dot{Q}_{2L} = \dot{Q}_{2aL} + \dot{Q}_{2bL} + \dot{Q}_{2cL} \quad (3)$$

In Eq. (3), $\dot{Q}_{2L}$ is the heat flow rate of the food, W; $\dot{Q}_{2bL}$ is the heat flow rate of the container box, W; and $\dot{Q}_{2cL}$ is the breathing heat of the food. For low-temperature storage, the breathing heat of the food is not considered, so =0W, then:

$$\dot{Q}_{2L} = \dot{Q}_{2aL} + \dot{Q}_{2bL} \quad (4)$$

High-temperature cold storage usually stores some fruit, vegetables and other cargo. For the heat flow rate of high-temperature storage goods:

$$\dot{Q}_{2H} = \dot{Q}_{2aH} + \dot{Q}_{2bH} + \dot{Q}_{2cH} \quad (5)$$

where $\dot{Q}_{2aH}$ is the heat flow rate of the food, W; $\dot{Q}_{2bH}$ is the heat flow rate of the container box, W; and $\dot{Q}_{2cH}$ is the breathing heat of fruit and vegetables.

For the fruit and vegetables in the high-temperature cold storage, they will still breathe heat when they are stored in the cold storage. Therefore, when calculating the heat flow rate of the high-temperature cold storage goods, the breathing heat of the fruits and vegetables needs to be considered, then:

$$\dot{Q}_{2H} = \dot{Q}_{2aH} + \dot{Q}_{2bH} + \dot{Q}_{2cH} \quad (6)$$

The heat flow rate $\dot{Q}_3$ generated when the cold storage door is opened for heat exchange

$$\dot{Q}_3 = \frac{nV\rho_o(h_1 - h_2) * 10^3}{24 * 3600} \quad (7)$$

where V is the capacity of the cold storage, m^3; is the enthalpy of the air outside the storage, kJ/kg; is the enthalpy of the air inside the cold storage, kJ/kg; n is the number of air changes in the 24 h internal cold storage; and ρ_o is the internal cold storage air density, kg/m^3.

Operating heat

$$\dot{Q}_4 = \dot{Q}_{4a} + \dot{Q}_{4b} + \dot{Q}_{4c} \quad (8)$$

$\dot{Q}_{4a}$ is the heat flow rate of the staff, W; $\dot{Q}_{4b}$ is the heat flow rate of the lighting equipment, W; $\dot{Q}_{4c}$ is the heat flow rate of the air cooler, W.

The cold storage is equipped with low-temperature cold storage and high-temperature cold storage. Usually the temperature of the low-temperature cold storage is -18°C to -20°C and the design temperature is -20°C; the temperature of the high-temperature cold storage is usually 0°C to -5°C, and the design temperature is 3°C. The outside temperature in summer is 30°C, the summer temperature in winter is 5°C and the outside temperature in spring and autumn is 15°C.

The heat flow rate of low-temperature cold storage and high-temperature cold storage in summer, winter, spring and autumn can be calculated. The specific values are shown in Table 4.

Tab. 4. Heat flow rate of high-temperature cold storage and low-temperature cold storage under different working conditions

Season	Load of low temperature cold storage (kW)	Load of high temperature cold storage (kW)
Summer	394.44	283.33
Winter	333.33	59.44
Spring and autumn	355.56	131.94

SPECIFIC SCHEME DESIGNS FOR DIFFERENT SAILING CONDITIONS

The 'CMA CGM JACQUES SAADE' serves Asian-European routes and the ship's voyage cycle is as long as 84 days, as shown in Table 5. Because of the long routes and the different latitudes of the ports it passes, the temperature along the route differs, and the same voyage will have different seasons. In addition, there are multiple ports of call in the voyage; in different port of call, the number of containers and types of goods are different, and the number of low temperature and high temperature cold storage is also different. Taking the above factors into consideration, combined with the cold storage's demand for cold energy and the total cold released by the system, Table 6 lists different combination schemes of low-temperature cold storage and high-temperature cold storage in different seasons.

Tab. 5. Sailing schedule for a certain voyage

Port	Arrival time	Departure time	Port	Arrival time	Departure time
Ningbo	March 3	March 7	Rotterdam	April 15	April 17
Yan Tian	March 9	March 10	Marsaxlokk	April 22	April 23
Singapore	March 17	March 18	Suez Canal	April 26	April 27
Suez Canal	March 29	March 30	Port Klang	May 6	May 8
Le Havre	April 5	April 7	Xin Gang	May 18	May 20
Dunkirk	April 8	April 9	Busan	May 22	May 24
Hamburg	April 12	April 14	Ningbo	May 25	May 26

Tab. 6. Combination scheme of the number of low temperature cold storage and high temperature cold storage

Conditions	Summer					Winter					Spring and autumn				
Scheme	S_1	S_2	S_3	S_4	S_5	S_6	S_7	S_8	S_9	S_{10}	S_{11}	S_{12}	S_{13}	S_{14}	S_{15}
Number of high temperature cold storage	1	1	2	1	2	3	3	2	2	3	2	2	3	2	3
Number of low temperature cold storage	2	3	1	1	0	4	2	3	2	0	3	2	1	1	0

SYSTEM SIMULATION

In order to verify the feasibility of the above 15 combination schemes, this study used Aspen HYSYS to carry out simulation calculations.

SELECTION OF REFRIGERANT

In order to ensure that the cold storage system can exchange heat normally and achieve a good heat transfer effect, a suitable refrigerant needs to be selected before the simulation, which can be selected according to the target temperature of different modules. Table 7 shows the target temperature range of different modules.

Tab. 7. Temperature range corresponding to different modules

Cold energy utilisation system	System temperature (°C)	The temperature range of the refrigerant (°C)
Intermediate refrigerant system	-40°C to -60°C	<-60°C
Low temperature cold storage system	Cold storage temperature -20°C to -18°C	≤-40°C
High temperature cold storage system	Cold storage temperature 0°C to -5°C	<-10°C

The selection of refrigerant must comply with the criteria for refrigerant selection. Whether the refrigerant is properly selected will affect the refrigeration effect and system performance of the cold storage. The cold storage system requires more cold energy. The selected refrigerant should have a large specific heat capacity, to carry the large amount of cold energy that will be generated if the refrigerant temperature change is too large, resulting in icing phenomenon. Because it is used for cold storage circulation, the refrigerant should not have a risk of burning or exploding, and its toxicity should be low because the refrigerant is used for cold storage circulation. The size of cold storage is large and the amount of refrigerant required is also large. Low-cost, easy-to-obtain, and quick-to-supply refrigerants should be selected, therefore, priority should be given to ethylene glycol aqueous solution, which is a more commonly used refrigerant. For high-temperature cold storage, the design temperature is 3°C, and the freezing point of the refrigerant is required to be <-10°C. 30% ethylene glycol aqueous solution is preferred and the freezing point of the glycol aqueous solution is -15°C, which meets the temperature requirements of high-temperature cold storage. For low-temperature cold storage, the design temperature is -20°C, the minimum freezing point of the refrigerant is required to be ≤-40°C, and the freezing point of 50% ethylene glycol aqueous solution is -40°C, which meets the temperature requirements for low-temperature cold storage. Therefore, the refrigerant in the low-temperature cold storage and the high-temperature cold storage are 30% and 50% ethylene glycol aqueous solution, respectively.

Low-temperature cold storage requires a lot of cold energy. The intermediate refrigerant should carry enough cold energy to ensure the normal operation of the system. Therefore, the intermediate refrigerant needs to undergo phase change, and the refrigerant undergoing phase change has a larger latent heat of phase change and a better heat transfer effect. Fig. 4 shows the condensation pressure curves of different refrigerants at different condensation temperatures.

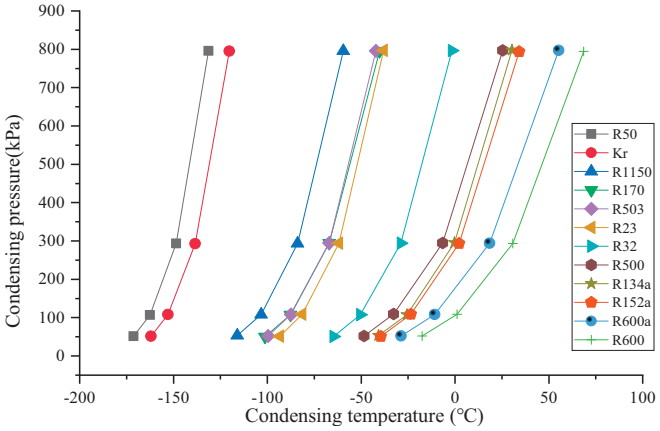

Fig. 4. Correspondence graph of condensation temperature and condensation pressure of different refrigerants

The intermediate refrigerant needs to undergo a phase change within the required temperature range of -40°C to -60°C. It can be seen from Fig. 4 that the refrigerants that meet the conditions are R23, R503, and R170. The main component of R23 is trifluoromethane, which is easily soluble in water, flammable and explosive, and has a high pressure. The safety level of the pipeline needs to be relatively high, and this refrigerant will release highly toxic fumes when heated and decomposed, so it is not suitable for cold storage systems. The main component of R170 is ethane, which is a hydrocarbon-carrying refrigerant and is more environmentally friendly. It often replaces R13 and R503 as a refrigerant, so R170 can be used as the intermediate refrigerant. The refrigerant is

a substance that easily evaporates. In the actual application process, in order to avoid this problem as much as possible, the sealing performance of the pipeline should be improved. The refrigerant may cause corrosion to the pipeline, so the pipeline material should be selected with corrosion resistance in mind.

DETERMINATION OF SIMULATION PARAMETERS

Assuming that the power unit of the 'CMA CGM JACQUES SAADE' LNG-powered container ship is operating at 70% load, it is calculated that, under this working condition, the LNG intake flow rate of the main engine is 6497 kg/h. Aspen HYSYS software was used for calculating the simulations of LNG and the physical property method of the refrigerant was Peng-Robinson. The physical property method of the jacket water was NBS Steam. The pump efficiency is 75% and the minimum heat exchange temperature difference of the heat exchanger was set at 8°C. 50% ethylene glycol aqueous solution was used as the low-temperature storage refrigerant, 30% ethylene glycol aqueous solution was used as the high-temperature cold storage refrigerant, and R170 was used as the intermediate refrigerant. In this simulation, it was assumed that the process is static and stable.

In order to avoid temperature crossing in the LNG heat exchanger, and to ensure that each cold energy utilisation system can meet the refrigeration requirements, the heat outlet temperature of the HEX-3 heat exchanger should be lower than the design temperature of the low-temperature cold storage (-20°C). It should not be lower than the inlet temperature of the cold flow (-30°C). In the same way, the hot flow outlet temperature of the HEX-4 heat exchanger should be 3°C lower than the design temperature of the high-temperature cold storage, and should not be lower than the cold flow inlet temperature (-5°C). According to the condensation pressure corresponding to the condensation temperature of the refrigerant in Fig. 4, the pressure of stream A-3 was set to 500 kPa. Taking Scheme 1 as an example, the main parameter settings in the system are shown in Table 8.

Tab. 8. Main parameter settings in the system

Stream name	Medium	P (kPa)	T (°C)	Flow (kg/h)
LNG-1	-	200	-163	6497
LNG-2	-	1600	-	-
NG-4	-	-	40	-
A-1	R170	-	-40	-
A-2	R170	-	-60	-
A-3	R170	500	-	-
B-1	Cylinder liner heating water	-	80	-
B-2	Cylinder liner heating water	-	68	-
C-2	50% ethylene glycol solution	-	-30	-
C-5	50% ethylene glycol solution	-	-20	-
D-2	30% ethylene glycol solution	-	-5	-
D-6	30% ethylene glycol solution	-	3	-
D-9	30% ethylene glycol solution	-	3	-

The parameter settings of other combination schemes are the same as the key node parameter settings of Scheme 1, and will not be repeated here. Taking Scheme 1 as an example, Fig. 5 is a diagram of the simulated system.

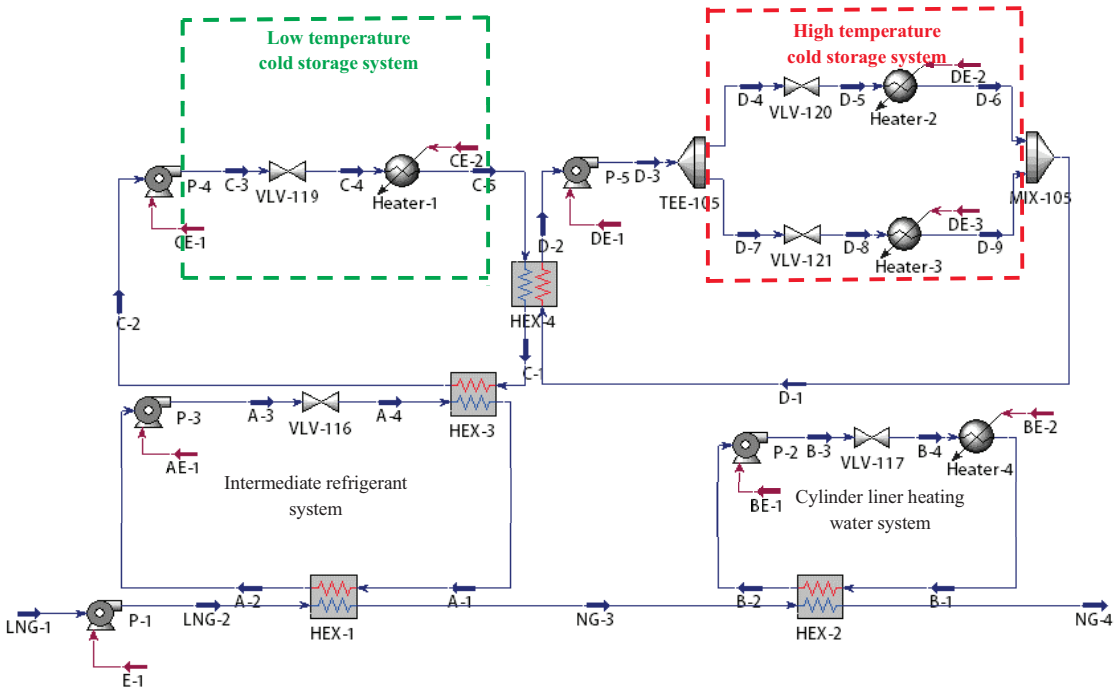

Fig. 5. LNG cold energy utilisation simulation system diagram

ANALYSIS OF SIMULATION RESULTS

Through the simulation, it can be seen that the 15 combination schemes of low and high temperature cold storage can all run normally in the Aspen HYSYS simulation.

(1) Exergy efficiency calculation model

Using Aspen HYSYS to simulate the system, the main parameters of each node of the system can be obtained, including temperature, pressure and flow, entropy, enthalpy, etc. Among these, the flow of the intermediate refrigerant in the cold storage system can be calculated by the known heat load. The flow rate of the jacket heating water in the jacket water heating system can also be calculated. Taking scheme 1 as an example, the important node parameters are shown in Table 9.

The exergy of logistics generally includes physical exergy and chemical exergy. In the process of cold energy utilisation, LNG mainly involves changes in physical form, mainly physical exergy changes. The cold energy utilisation system proposed in this paper is a stable flow system. For a stable flow system, according to the first law of thermodynamics:

$$\delta Q = dH + \frac{1}{2}mdc^2 + mgdz + \delta W_A \tag{9}$$

From the second law of thermodynamics,

$$\delta Q = T_0 ds \tag{10}$$

Therefore,

$$T_0 ds = dH + \frac{1}{2}mdc^2 + mgdz + \delta W_A \tag{11}$$

$$\delta W_A = -dH + T_0 ds - \frac{1}{2}mdc^2 - mgdz \tag{12}$$

Therefore, in the environmental state, from a given import state integral to an export state integral, the exergy of stable logistics is:

$$E_{xmass} = W_A = H - H_0 - T_0(S - S_0) + \frac{1}{2}mdc^2 + mgdz \tag{13}$$

Since the kinetic and potential energy of the logistics in the cold energy utilisation system have small changes and can be ignored, the calculation formula for the exergy of the stable flow system logistics is:

$$E_{xmass} = W_A = H - H_0 - T_0(S - S_0) \tag{14}$$

Therefore,

$$E_{xmass} = m[(h - h_0) - T_0(s - s_0)] \tag{15}$$

In the formula: m is the mass flow of each stream and h and s are the enthalpy and entropy of each flow, respectively.

The power consumption of the working fluid pump is:

$$\mathcal{W}_p = \frac{m\left(h_0^{'} - h_i^{'}\right)}{\eta_p} \tag{16}$$

In the formula: η_p is the isentropic efficiency of the pump; $h_i^{'}$ is the enthalpy value of the pump inlet flow; and h_0 is the enthalpy value of the pump outlet flow.

Tab. 9. The main simulation results parameters of scheme 1

Stream name	Flow (kg/h)	T (°C)	P (kPa)	s (kJ/kgK)	h (kJ/kg)
LNG-1	6497	-163	200	4.461	-5240
NG-4	6497	40	1560	9.604	-4336
B-1	47180	80	120	1.075	-15590
B-2	47180	68	100	0.930	-15640
B-3	47180	68.03	300	0.931	-15640
B-4	47180	68.03	280	0.931	-15640
A-1	7278	-40	460	6.384	-2934
A-2	7278	-60	440	4.200	-3411
C-1	51300	-5.863	240	-15.390	-9932
C-2	51300	-30	220	-15.890	-9400
C-5	51300	-20	260	-15.660	-9372
D-1	80790	3	260	-2.028	-10830
D-2	80790	-5	240	-24.580	-10850

In this study, the exergy efficiency is used as an indicator to evaluate the energy utilisation of the system, because the exergy efficiency can reflect the ability of the system to perform external work. The system uses LNG cold energy to refrigerate the ship's cold storage, which can save the power consumption of the refrigerated container refrigeration unit. This reduces the load of the ship's power grid, so it can be considered that the system is doing external work. In addition, the system uses LNG cold energy to refrigerate the ship's cold storage, which belongs to heat exchange and refrigeration. Therefore, the utilisation rate of LNG cold energy can also be used as another indicator to evaluate the energy utilisation of the system.

The exergy efficiency ε is the ratio of the effective income exergy to the consumption exergy. In this study, effective exergy E_{CS} is the exergy input from the working medium of cold storage to the environment of low temperature cold storage and high temperature cold storage. If the pump power consumption (W_p), the LNG cold exergy consumed (E_{LNG}–E_{NG-4}) and the exergy of the jacket water (E_F) are used as the

consumption exergy, then the exergy efficiency calculation model of the system is:

$$\varepsilon = \frac{E_{cs}}{\mathcal{W}_p + E_{LNG-1} - E_{NG-4} + E_F} \tag{17}$$

The values obtained through Aspen HYSYS can be put into equations Eq. (15) and (16), respectively, to work out the exergy of flows of each part and the power consumption of the pump. Then, the corresponding calculated values can be put into Eq. (17) and the exergy efficiency of the system under various schemes can be obtained.

(2) Calculation model of the cold energy utilisation rate

The utilisation rate of cold energy can be used to measure the utilisation of cold energy by the system. The utilisation rate of cold energy η is the ratio of the effective utilisation of cold energy to the total cold energy released by the system. The cold energy utilisation in this study is the cold energy consumed by low-temperature cold storage and high-temperature cold storage, Q_{CS}, and the total cold energy is the cold energy, Q_{LNG}, released by the vapourisation of LNG. The calculation model of the cold energy utilisation rate of the system is:

$$\eta = \frac{Q_{cs}}{Q_{LNG}} \tag{18}$$

According to the different combination schemes of low-temperature cold storage and high-temperature cold storage, under different working conditions, the total cooling capacity required by the cold storage can be calculated under different combination schemes. Bringing the calculated value into Eq. (18) can find the cold energy utilisation rate of different combination schemes under different working conditions.

(3) Summary of results

According to the different schemes listed in Table 6, the exergy efficiency and cold energy utilisation rate of different schemes can be calculated for different seasons. The calculated results are shown in Fig. 6.

From Fig. 6(a), it can be seen that, in summer conditions, the system of scheme 3 (2 low-temperature cold storage and 1 high-temperature cold storage) has the highest exergy efficiency, which can reach 45.41%. The corresponding cold energy utilisation rate is 69.93%. Scheme 2 (1 low-temperature cold storage, 3 high-temperature cold storage) has the highest cold energy utilisation rate, which can reach 81.16%, and the corresponding system's exergy efficiency is 43.31%. From Fig. 6(b), it can be seen that, in winter conditions, scheme 6 (3 low-temperature cold storages, 4 high-temperature cold storages) and scheme 7 (3 low-temperature cold storages, 2 high-temperature cold storages) have the highest exergy efficiency, which can reach 49.45%, and the cold energy utilisation rate of scheme 6 is the highest, at 80.72%. It can be seen from Fig. 6(c) that, in the spring and autumn conditions, the exergy efficiency of the system of scheme 13 (3 low temperature storage and 1 high temperature storage) is the highest, which can reach 48.80%, and the cold energy utilisation rate is also the highest at this time (78.17%).

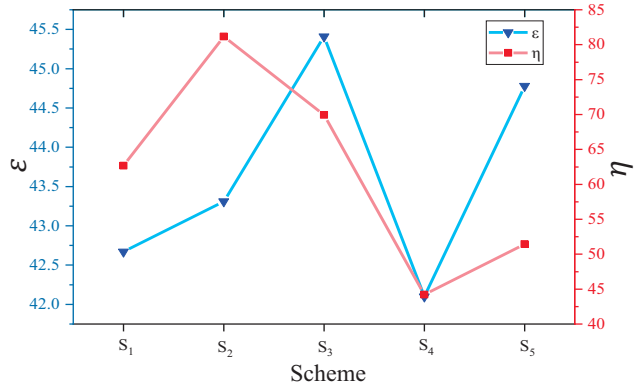

(a) Summer conditions

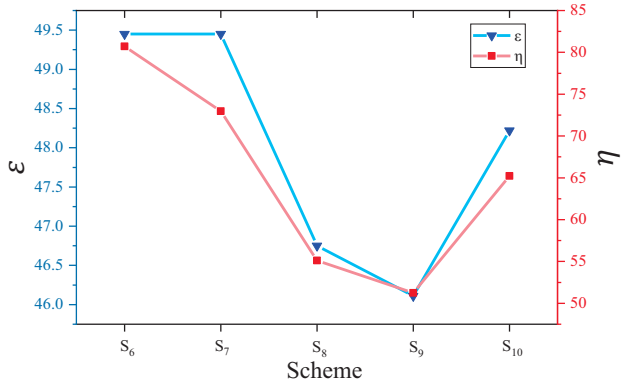

(b) Winter conditions

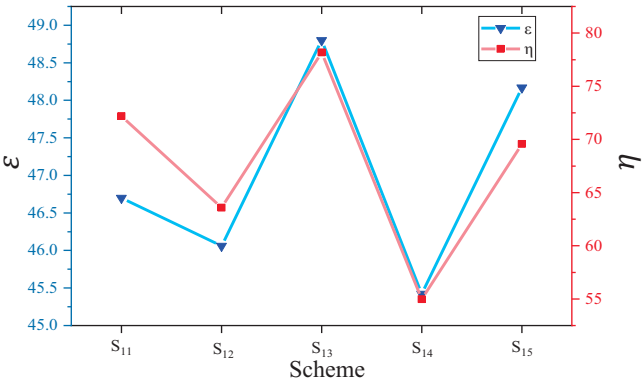

(c) Spring and autumn conditions

Fig. 6. The exergy efficiency of the system and the cold energy utilisation rate of the system under different combination schemes

ANALYSIS OF ACTUAL ROUTE APPLICATION

EXERGY EFFICIENCY AND COLD ENERGY UTILISATION RATE

Tab. 10. Different departure times at the starting port

T	T_1	T_2	T_3	T_4	T_5	T_6	T_7	T_8
Departure time	March 3	April 28	June 2	July 28	September 2	October 28	December 2	January 27

Based on the characteristics of cross-seasonal navigation of LNG-powered container ships, different combination schemes of low-temperature cold storage and high-temperature cold storage are proposed for different seasons. Aspen HYSYS software is used to simulate and calculate the different combination schemes of the system. According to the simulation results, the exergy efficiency and cold energy utilisation rate of the system under different combination schemes can be obtained. In order to explore the utilisation of LNG cold energy during actual navigation of this type of ship, the different departure times at the starting port are listed. They are marked as T_1-T_8 and the specific departure times are shown in Table 10.

When a ship sails between two adjacent ports on the route, it is affected by the type and quantity of local cargo, the different number of containers, and the changing number of low-temperature cold storage and high-temperature cold storage required. According to actual research, the number of refrigerated containers between two adjacent ports can be obtained. According to Table 6, the combination of high-temperature cold storage and low-temperature cold storage between two adjacent ports can be selected, as shown in Table 11. For the convenience of presentation, Ningbo (A), Yantian (B), Singapore (C), Suez Canal (D), Le Havre (E), Dunkirk (F), Hamburg (G), Rotterdam (H), Marsaschloch (I), Suez Canal (J), Port Klang (K), Tianjin Xingang (L), and Busan (M) call ports are recorded as A-M, respectively. Among them, in the table, n represents the number of containers, unit 10^3; n_L represents the number of low-temperature cold storage, unit: piece; n_H represents the number of high-temperature cold storage, unit: piece; and S represents the combination scheme adopted.

Tab. 11. Schemes of low-temperature cold storage and high-temperature cold storage under different conditions

Port \ T		T_1	T_2	T_3	T_4	T_5	T_6	T_7	T_8	Port \ T		T_1	T_2	T_3	T_4	T_5	T_6	T_7	T_8
A-B	n	1.1	1	1	1	1	1	1	1	G-H	n_H	2	1	2	2	2	2	2	2
	n_L	2	2	2	2	1	2	2	2		S	S_9	S_{13}	S_{12}	S_{12}	S_{12}	S_9	S_9	S_9
	n_H	3	1	1	1	3	2	2	2	H-I	n	0.85	0.80	0.95	0.85	0.95	0.85	0.85	0.85
	S	S_{11}	S_3	S_3	S_3	S_2	S_{12}	S_{12}	S_{12}		n_L	3	2	3	3	2	2	2	3
B-C	n	1.3	1.3	1.3	1.3	1.3	1.3	1.3	1.3		n_H	0	1	0	1	2	2	2	1
	n_L	1	1	1	1	1	1	1	1		S	S_{10}	S_{14}	S_{15}	S_{13}	S_{12}	S_{12}	S_9	S_{13}
	n_H	3	2	2	3	3	3	3	3	I-J	n	0.70	0.68	0.80	0.70	0.80	0.70	0.70	0.70
	S	S_2	S_1	S_1	S_2	S_2	S_2	S_2	S_2		n_L	2	2	1	2	2	2	3	2
C-D	n	1.5	1.5	1.5	1.5	1.5	1.5	1.5	1.5		n_H	1	1	0	1	1	1	0	1
	n_L	1	1	1	1	1	1	1	1		S	S_3	S_3	S_1	S_{14}	S_3	S_{14}	S_{10}	S_3
	n_H	3	3	3	3	3	3	3	3	J-K	n	0.70	0.68	0.80	0.70	0.80	0.70	0.70	0.70
	S	S_2	S_2	S_2	S_2	S_2	S_2	S_2	S_2		n_L	2	2	1	2	2	2	3	2
D-E	n	1.5	1.5	1.5	1.5	1.5	1.5	1.5	1.5		n_H	1	1	2	1	1	1	0	1
	n_L	1	1	1	1	1	2	2	2		S	S_3	S_3	S_1	S_3	S_3	S_{14}	S_{15}	S_3
	n_H	3	3	3	3	3	3	3	3	K-L	n	0.45	0.55	0.55	0.50	0.60	0.50	0.50	0.50
	S	S_2	S_2	S_2	S_2	S_2	S_{11}	S_{11}	S_{11}		n_L	1	2	2	1	2	2	1	1
E-F	n	1.40	1.40	1.35	1.40	1.40	1.40	1.40	1.40		n_H	1	0	1	1	1	1	1	1
	n_L	2	2	2	2	2	2	3	2		S	S_4	S_5	S_3	S_4	S_{14}	S_{14}	S_4	S_4
	n_H	3	3	3	3	3	3	4	3	L-M	n	0.38	0.38	0.45	0.40	0.45	0.40	0.40	0.40
	S	S_{11}	S_{11}	S_{11}	S_{11}	S_{11}	S_{11}	S_6	S_{11}		n_L	2	1	1	2	3	3	2	2
F-G	n	1.30	1.30	1.28	1.30	1.30	1.30	1.30	1.30		n_H	1	1	0	1	0	0	1	1
	n_L	3	2	3	2	2	3	3	3		S	S_3	S_4	S_5	S_{14}	S_{10}	S_{10}	S_{14}	S_{14}
	n_H	2	2	1	3	3	2	2	2	M-A	n	320	300	350	300	380	300	300	300
	S	S_7	S_{12}	S_{13}	S_{11}	S_{11}	S_7	S_7	S_7		n_L	2	2	1	2	1	3	2	3
G-H	n	1.00	1.08	1.10	1.00	1.10	1.00	1.00	1.00		n_H	0	0	1	1	1	0	1	0
	n_L	2	3	2	2	2	2	2	2		S	S_{14}	S_{10}	S_{14}	S_{15}	S_{14}	S_{10}	S_{14}	S_{15}

According to the research above, the parent ship may need to complete the switch between the low-temperature cold storage and the high-temperature cold storage in a certain port due to the change in the combination schemes of low-temperature cold storage and high-temperature cold storage. In actual applications, it is relatively easy to complete this process by valve control, as shown in Fig. 7. If it is assumed that cold storage 1 is a low-temperature cold storage at the beginning and cold storage 2 is a high-temperature cold storage, valves 1, 4, 3, and 6 are opened, and valves 2, 5 are closed, then the high-temperature cold storage needs to be turned into a low-temperature cold storage. Valves 1, 2, 4 and 5 are opened and valves 3 and 6 are closed so that the transition from a high-temperature cold storage to a low-temperature cold storage can be completed. The transition from a low-temperature cold storage to a high-temperature cold storage can also be completed in the same way. In the actual application process, when switching between high-temperature cold storage and low-temperature cold storage, refrigerants of different concentrations may be mixed, but because the amount of refrigerant is relatively small, this will not have much impact on the normal operation of the system. In addition, the sealing performance of the pipeline should be strengthened to prevent the leakage of the refrigerant.

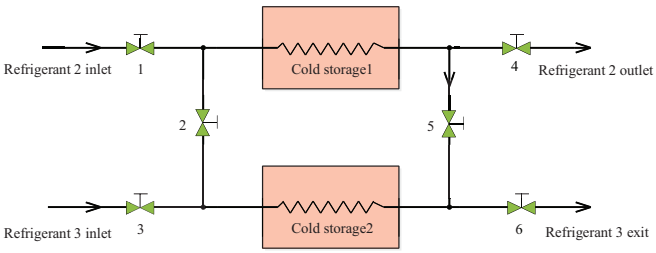

Fig. 7. System diagram of low-temperature cold storage and high-temperature cold storage switching

According to the combination schemes of low-temperature cold storage and high-temperature cold storage selected between two adjacent ports at different departure times of the starting port listed in Table 11. The exergy efficiency and cold energy utilisation rate of the system between two adjacent ports on the entire route are summarised in Fig. 8 and Fig. 9.

It can be seen from Fig. 9 and Fig. 10 that the exergy efficiency and cold energy utilisation rate of the system between adjacent ports change dynamically. The number of refrigerated containers in different ports and the number of low-temperature cold storage and high-temperature cold storage are different. Therefore, the combination schemes of low-temperature cold storage and high-temperature cold storage used between two adjacent ports is also different.

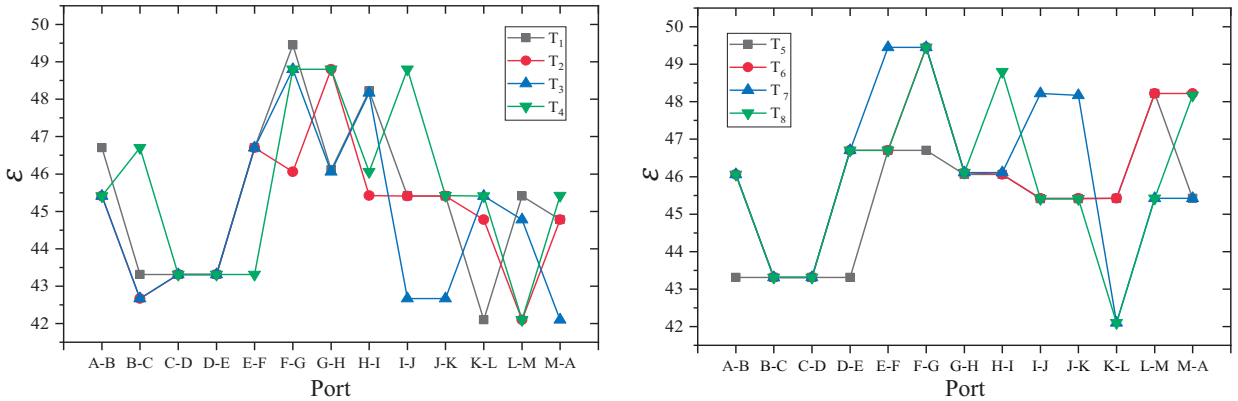

(a)T_1-T_4 (b)T_5-T_8

Fig. 8. Exergy efficiency of the system at different departure times from the starting port

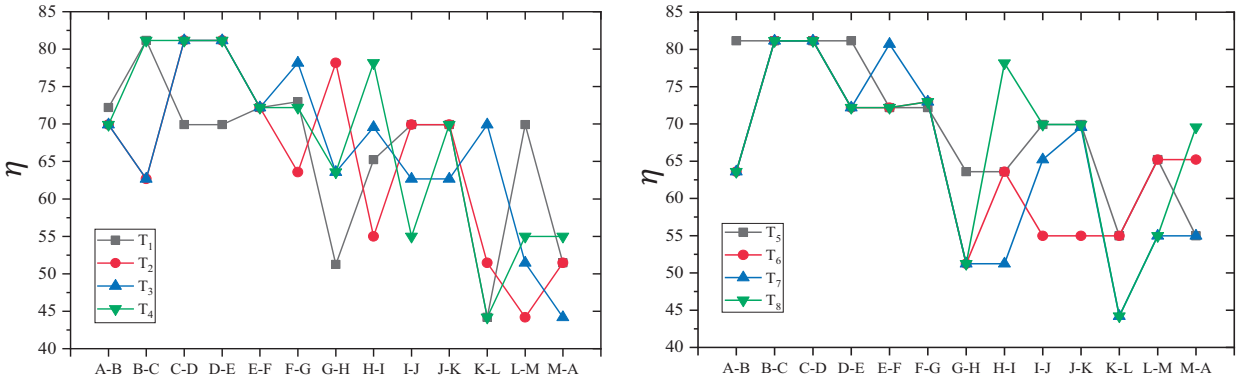

(a)T_1-T_4 (b)T_5-T_8

Fig. 9. Cold energy utilisation rate of the system at different departure times from the starting port

As a result, the system's exergy efficiency and cold energy utilisation rate change dynamically along the entire route.

In order to better evaluate the utilisation of cold energy by the system during the entire voyage, according to the system's exergy efficiency and cold energy utilisation rate between two adjacent ports on the route, the average exergy efficiency and average cold energy utilisation rate of the system along the entire route are calculated. The results are shown in Fig. 10.

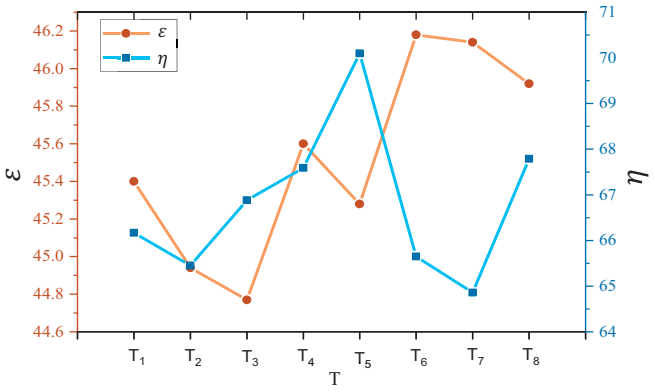

Fig. 10. The average exergy efficiency and average cold energy utilisation rate of the system along the entire route

Fig. 10 shows that the highest average exergy efficiency and average cold energy utilisation rate of the system along the entire route are 46.18% and 70.10%, respectively; the lowest average exergy efficiency and average cold energy utilisation rate of the system are 44.77% and 64.86%, respectively. It can be seen that if an LNG-powered container ship adopts the LNG cold energy utilisation system proposed in this study, then it can effectively utilise LNG cold energy.

ECONOMIC ANALYSIS

The LNG cold energy utilisation method proposed in this study will reduce part of the electrical energy of the ship's power grid that is consumed by refrigerated container refrigeration, but when the ship calls at a port or the LNG cold energy is not enough to ensure the refrigeration of all the refrigerated containers in the cold storage, it is necessary to consume the electric energy of the ship's power grid and use refrigeration equipment to refrigerate a single refrigerated container. According to actual investigations, the average power of a 40-foot refrigerated container during continuous refrigeration operation is between 4.8 kW and 5.8 kW. In this study, the electric energy consumed by the refrigerated containers before and after the cold storage refrigeration was calculated by using the LNG cold energy during the entire voyage period, corresponding to the different departure times at the starting port. The calculated results are denoted as and , respectively. The calculated results are shown in Fig. 11. The amount of fuel saved q can be calculated from the saved electric energy and, thus, the reduced carbon emissions Mc can be calculated from the saved amount of fuel. The calculated results are shown in Fig. 12.

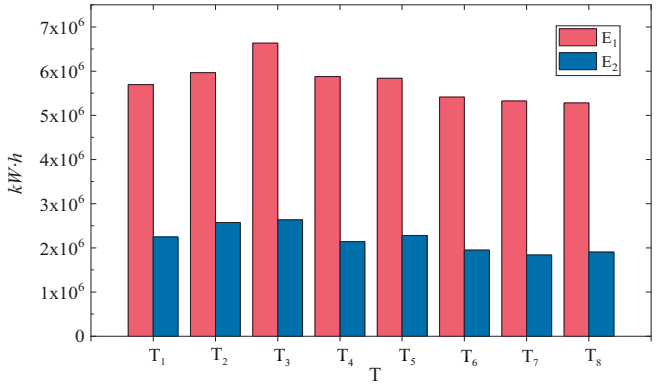

Fig. 11. Comparison of cold storage power consumption at different departure times from the starting port

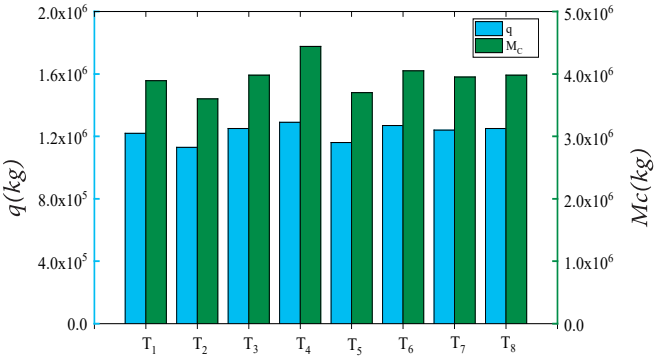

Fig. 12. Fuel saving and carbon emission reduction at different departure times from the port of origin

It can be seen from Fig. 11 and 12 that the electric energy consumption of refrigeration equipment is significantly reduced after the use of LNG cold energy to refrigerate the cold storage. Along the entire route, the maximum electric energy can be reduced by $7.14*10^6$ kW·h, which is equivalent to saving $1.29*10^6$ kg of fuel, reducing $4.44*10^6$ kg of carbon emissions and improving the energy utilisation rate of the whole ship. This accords with the general trend of energy saving and emission reduction and has good value in its practical application.

CONCLUSIONS

In order to solve the problems of excessive LNG cold energy and large power consumption of refrigerated containers on LNG-powered container ships, this study proposed a new utilisation method that uses LNG cold energy to cool refrigerated containers in the cargo hold of ships. According to the actual operating conditions of the ship and the characteristics of the route, different combination schemes of the number of low-temperature cold storage and high-temperature cold storage units are designed. Exergy efficiency and cold energy utilisation rates of different combination schemes were calculated by Aspen HYSYS software and the economic efficiency of the cold energy utilisation system of

LNG fuel along the whole route was evaluated and analysed; the conclusions were as follows:

1. This research proposes a new utilisation method for using the cold energy of LNG-powered container ships for refrigerated containers. On this basis, a new type of cold storage using LNG cold energy was designed and the low-temperature cold storage and high-temperature cold storage models were further established. The main structure of the new cold storage was modelled in three dimensions and finally realised the cascade utilisation of LNG fuel cold energy, which can effectively solve the problem of excess cold fuel energy on LNG-powered ships, improve the energy utilisation rate and improve the economy of the ships. It has a very good practical significance to realise the energy saving and emission reduction of ships.

2. This study designed the number of low-temperature cold storage and high-temperature cold storage units under different seasonal conditions, according to the heat load of the cold storage of the parent ship in different seasons, combined with the total cold released by the ship during navigation. 15 different low-temperature cold storage and high-temperature cold storage combinations were investigated as optimal schemes.

3. Aspen HYSYS software was used to establish a new LNG-powered ship's cold energy utilisation process and set the parameters of key nodes in it to obtain the parameters of each node. The calculation model of the system's exergy efficiency and cold energy utilisation rate under different combination schemes was established and the exergy efficiency and cold energy utilisation rate of the new utilisation method was calculated. It can be concluded that the highest exergy efficiency of the system in the 15 combination schemes reached 49.45%, and the highest cold energy utilisation rate reached 81.16%, which provides theoretical support for evaluating the exergy efficiency and cold energy utilisation rate of the system along the entire route.

4. In order to get close to the actual sailing situation of the ship, this research is based on the characteristics of the ship's cross-seasonal navigation, regarding the different departure times at the starting ports and the number of refrigerated containers between two adjacent ports (the combination schemes of the number of low-temperature cold storage and high-temperature cold storage was selected for it). The average exergy efficiency and cold energy utilisation rate of the system along the entire route were summarised. It was found that the average exergy efficiency and average cold energy utilisation rate of the system were at their lowest at 44.77% and 64.86%, respectively, which proved that this type of ship can effectively utilise LNG cold energy.

5. This study calculates the total electrical energy consumed by refrigerated containers along the entire route before and after using the LNG cold energy utilisation method. It was found that, after adopting the new cold energy utilisation method, the power consumption for refrigerated container refrigeration was significantly reduced, and the power consumption could be reduced by $7.14*10^6$ kW·h, which was equivalent to saving $1.29*10^6$ kg of fuel and $4.44*10^6$ kg of carbon emissions. It can be seen that the LNG cold energy utilisation method proposed in this study has a promoting effect on the green development of ships.

ACKNOWLEDGEMENTS

The project was funded by Natural Science Foundation of Shandong Province of China (ZR2021ME156), Tsinghua University Shuimu Scholar Program (2020SM027) and China Postdoctoral Science Foundation (BX20200187, 2021M691718).

REFERENCES

1. X. Gu, G. Jiang, Z. Guo, and S. Ding, 'Design and Experiment of Low-Pressure Gas Supply System for Dual Fuel Engine', Polish Marit. Res., vol. 27, no. 2, 2020, doi: 10.2478/pomr-2020-0029.

2. O. Cherednichenko, S. Serbin, and M. Dzida, 'Application of Thermo-chemical Technologies for Conversion of Associated Gas in Diesel-Gas Turbine Installations for Oil and Gas Floating Units', Polish Marit. Res., vol. 26, no. 3, 2019, doi: 10.2478/pomr-2019-0059.

3. S. Serbin, B. Diasamidze, and M. Dzida, 'Investigations of the working process in a dual-fuel low-emission combustion chamber for an fpso gas turbine engine', Polish Marit. Res., vol. 27, no. 3, 2020, doi: 10.2478/pomr-2020-0050.

4. T.C. Van, J. Ramirez, T. Rainey, et al. 'Global impacts of recent IMO regulations on marine fuel oil refining processes and ship emissions', Transportation Research Part D, vol. 70, 2019, doi: 10.1016/j.trd.2019.04.001.

5. L.P Perera, and B. Mo, 'Emission Control Based Energy Efficiency Measures in Ship Operations', Applied Ocean Research, vol. 60, 2016, doi: 10.1016/j.apor.2016.08.006.

6. H.P. Nguyen, A.T. Hoang, S. Nizetic, et al. 'The electric propulsion system as a green solution for management strategy of CO2 emission in ocean shipping: A comprehensive review', International Transactions on Electrical Energy Systems, 2020, doi: 10.1002/2050-7038.12580.

7. N.R. Sharma, D. Dimitrios, A.I. Ler, et al. 'LNG a clean fuel the underlying potential to improve thermal efficiency', Journal of Marine Engineering & Technology, 2020, doi: 10.1080/20464177.2020.1827491.

8. I. Mallidis, S. Despoudi, R. Dekker, et al. 'The impact of sulphur limit fuel regulations on maritime supply chain network design', Annals of Operations Research, vol. 294, no. 8, 2018, doi: 10.1007/s10479-018-2999-4.

9. L.B. Reinhardt, D. Pisinger, M.M. Sigurd, et al. 'Speed optimizations for liner networks with business constraint', European Journal of Operational Research, vol. 285, no. 3, 2020, doi: 10.1016/j.ejor.2020.02.043.

10. Eun, Soo, and Jeong, 'Optimization of power generating thermoelectric modules utilizing LNG cold energy', Cryogenics, vol. 88, 2017, doi: 10.1016/j.cryogenics.2017.10.005.

11. O. Schinas, and M. Butler, 'Feasibility and commercial considerations of LNG-fueled ships', Ocean Engineering, vol. 122, 2016, doi: 10.1016/j.oceaneng.2016.04.031.

12. R. Zhao et al., 'A Numerical and Experimental Study of Marine Hydrogen-Natural Gas-Diesel Tri-Fuel Engines', Polish Marit. Res., vol. 27, no. 4, 2020, doi: 10.2478/pomr-2020-0068.

13. M. Badami, J.C. Bruno, A. Coronas, and G. Fambri, 'Analysis of different combined cycles and working fluids for LNG exergy recovery during regasification', Energy, vol. 159, 2018, doi: 10.1016/j.energy.2018.06.10.

14. B.B. Kanbur, L. Xiang, S. Dubey, F.H. Choo, and F. Duan, 'Cold utilisation systems of LNG: a review', Renewable and Sustainable Energy Reviews, vol. 79, 2017, doi: 10.1016/j.rser.2017.05.161.

15. J. Dong, S. Huang, S. Li, Y. Yao, Y. Jiang, 'LNG cold energy used in cold storage refrigeration performance simulation research', Journal of Harbin Institute of Technology, vol. 49, no. 2, 2017.

16. T. Banaszkiewicz, 'The Possible Coupling of LNG Regasification Process with the TSA Method of Oxygen Separation from Atmospheric Air', Entropy, vol. 23, no. 3, 2021, doi: 10.3390/e23030350.

17. W. Lin, M. Huang, H. He, et al., 'A transcritical CO2 Rankine Cycle with LNG cold energy utilisation and liquefaction of CO2 in gas turbine exhaust', Journal of Energy Resources Technology, vol. 131, no. 4, 2009, doi: 10.1115/1.4000176.

18. T. Jin, J.J. Hu, G.B. Chen, and K. Tang, 'Novel air separation unit cooled by liquefied natural gas cold energy and its performance analysis', Journal of Zhejiang University, vol. 41, no. 5, 2007.

19. E. Baldasso, M.E. Mondejar, S. Mazzoni, et al., 'Potential of liquefied natural gas cold energy recovery on board ships', Journal of Cleaner Production, vol. 271, 2020, doi: 10.1016/j.jclepro.2020.122519.

20. H.L. Sang, and K. Park, 'Conceptual design and economic analysis of a novel cogeneration desalination process using LNG based on clathrate hydrate', Desalination, vol. 498, 2021, doi: 10.1016/j.desal.2020.114703.

21. P. Babu, A. Nambiar, R.C. Zheng, et al., 'Hydrate-based desalination (HyDesal) process employing a novel prototype design', Chemical Engineering Science, vol. 218, 2020, doi: 10.1016/j.ces.2020.115563.

22. J. Sun, K. Han, C. Xie, et al., 'Liquid-solid fluidized bed seawater ice desalination based on LNG cold energy'. Modern Chemical Industry, vol. 40, no. 7, 2020, doi: 10.16606/j.cnki.issn0253-4320.2020.07.042.

23. I.M. Mujtaba, W. Cao, and C. Beggs, 'Theoretical approach of freeze seawater desalination on flake ice maker utilizing LNG cold energy', Desalination, vol. 355, 2015, doi: 10.1016/j.desal.2014.09.034.

24. E.G. Cravalho, J.J. McGrath, and W.M. Toscano, 'Thermodynamic analysis of the regasification of LNG for the desalination of sea water', Cryogenics, vol. 17, no. 3, 1977, doi: 10.1016/0011-2275(77)90272-7.

25. T. He, R. Zheng, J. Zheng, Y. Ju, et al., 'LNG cold energy utilisation: prospects and challenges', Energy, vol. 170, 2019, doi: 10.1016/j.energy.2018.12.170.

26. N. Yamanouchi, and H. Nagasawa, 'Using LNG cold for air separation', Chemical Engineering Progress, vol. 75, no. 7, 1979.

27. Y. Wu, Y. Xiang, L. Cai, et al., 'Optimization of a novel cryogenic air separation process based on cold energy recovery of LNG with exergoeconomic analysis', Journal of Cleaner Production, vol. 275, 2020, doi: 10.1016/j.jclepro.2020.123027.

28. M. Mehrpooya, B. Golestani, and S. Mousavian, 'Novel cryogenic argon recovery from the air separation unit integrated with LNG regasification and CO2 transcritical power cycle', Sustainable Energy Technologies and Assessments, vol. 40, no. 3, 2020, doi: 10.1016/j.seta.2020.100767.

29. R. Zhang, C. Wu, W. Song, et al., 'Energy integration of LNG light hydrocarbon recovery and air separation: Process design and technic-economic analysis', Energy, vol. 207, 2020, doi: 10.1016/j.energy.2020.118328.

30. Z. Gu, 'The simulation and operation optimization of the C_2~+ recovery process from LNG', Petrochemical Industry Application, vol. 37, no. 4, 2018.

31. T. Gao, W. Lin, and A. Gu, 'Improved processes of light hydrocarbon separation from LNG with its cryogenic energy utilised', Energy Conversion & Management, vol. 52, no. 6, 2011, doi: 10.1016/j.enconman.2010.12.040.

32. T. Yamamoto, T. Furuhata, N. Arai, and K. Mori, 'Design and testing of the Organic Rankine Cycle', Energy, vol. 26, no. 3, 2001.

33. N.B. Desai and S. Bandyopadhyay, 'Process integration of organic Rankine cycle', Energy, vol. 34, no. 10, 2009, doi: 10.1016/j.energy.2009.04.037.

34. J. Koo, S.R. Oh, Y.U. Choi, et al., 'Optimization of an Organic Rankine Cycle System for an LNG-Powered Ship', Energies, doi: 10.3390/en12101933.

35. Z. Tian, W. Zeng, B. Gu, et al., 'Energy, exergy, and economic (3E) analysis of an organic Rankine cycle using zeotropic mixtures based on marine engine waste heat and LNG cold energy', Energy Conversion and Management, vol. 228, 2020, doi: 10.1016/j.enconman.2020.113657.

36. X. Sun, S. Yao, J. Xu, et al., 'Design and Optimization of a Full-Generation System for Marine LNG Cold Energy Cascade Utilisation', Journal of Thermal Science, vol. 29, no. 3, 2020, doi: 10.1007/s11630-019-1161-1.

37. L. Xu, and G. Lin, 'LNG-FSRU new LNG cold energy power generation optimization plan', Natural gas chemical industry (C1 chemistry and chemical engineering), vol. 45, no. 5, 2020.

38. L. Zhao, J. Zhang, X. Wang, et al., 'Dynamic exergy analysis of a novel LNG cold energy utilisation system combined with cold, heat and power', Energy, vol. 212, 2020, doi: 10.1016/j.energy.2020.118649.

39. I.A. Fernández, M.R. Gómez, J.R. Gómez, and L.M. López-González, 'Generation of H2 on Board Lng Vessels for Consumption in the Propulsion System', Polish Marit. Res., vol. 27, no. 1, 2020, doi: 10.2478/pomr-2020-0009.

CONTACT WITH THE AUTHORS

Boyang Li
e-mail: qdlby@126.com

College of Electromechanical Engineering,
Qingdao University of Science and Technology,
Qingdao, 266061 Qingdao,
China

Yajing Li
e-mail: sdliyajing@126.com

China
College of Electromechanical Engineering,
Qingdao University of Science and Technology,
Qingdao, 266061 Qingdao,
China

Fang Deng
e-mail: dengfhelen@163.com

College of Electromechanical Engineering,
Qingdao University of Science and Technology,
Qingdao, 266061 Qingdao,
China

Qianqian Yang
e-mail: sdqdyqq@126.com

College of Electromechanical Engineering,
Qingdao University of Science and Technology,
Qingdao, 266061 Qingdao,
China

Baoshou Zhang
e-mail: sxsdzbs@126.com

School of Aerospace Engineering,
Tsinghua University,
Beijing, 100084 Beijing,
China